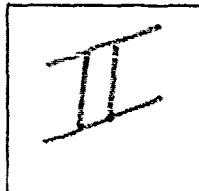


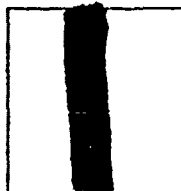
PHOTOGRAPH THIS SHEET

ADA090001

DTIC ACCESSION NUMBER



LEVEL



INVENTORY

Hawaii Univ. (Honolulu)
Dept. of Physics and Astronomy

Technical Report No. 003

DOCUMENT IDENTIFICATION

Dtd. 30 April 1980

Contract No. N00014-78-C-0417

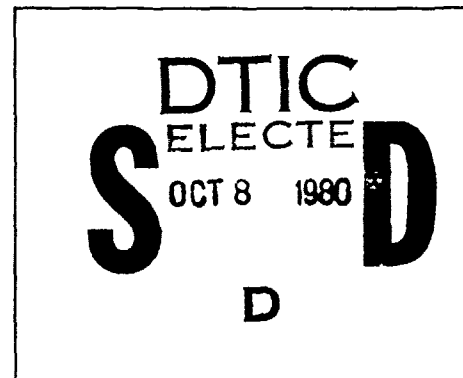
DISTRIBUTION STATEMENT A

Approved for public release;
Distribution Unlimited

DISTRIBUTION STATEMENT

ACCESSION FOR	
NTIS	GRA&I
DTIC	TAB
UNANNOUNCED	
JUSTIFICATION	
BY	
DISTRIBUTION /	
AVAILABILITY CODES	
DIST	AVAIL AND/OR SPECIAL
A	

DISTRIBUTION STAMP



DATE ACCESSIONED

80 10 1 027

DATE RECEIVED IN DTIC

PHOTOGRAPH THIS SHEET AND RETURN TO DTIC-DDA-2

AD A090001

TECHNICAL REPORT: 003

ANGULAR DEPENDENCE OF LIQUID CRYSTAL BASED
NEMATIC ACOUSTIC FIELD IMAGING DEVICES

C. F. HAYES

DEPARTMENT OF PHYSICS AND ASTRONOMY

UNIVERSITY OF HAWAII

HONOLULU, HAWAII 96822

APRIL, 1980

UNCLASSIFIED

REPORT DOCUMENTATION PAGE		READ INSTRUCTIONS BEFORE COMPLETING FORM
1. REPORT NUMBER 003	2. GOVT ACCESSION NO.	3. RECIPIENT'S CATALOG NUMBER
4. TITLE (and Subtitle) ANGULAR DEPENDENCE OF LIQUID CRYSTAL BASED NEMATIC ACOUSTIC FIELD IMAGING DEVICES		5. TYPE OF REPORT & PERIOD COVERED Technical Report (April, 1980)
		6. PERFORMING ORG. REPORT NUMBER
7. AUTHOR(s) Charles F. Hayes		8. CONTRACT OR GRANT NUMBER(s) N00014-78-C-0417
9. PERFORMING ORGANIZATION NAME AND ADDRESS Department of Physics and Astronomy University of Hawaii Honolulu, Hawaii 96822		10. PROGRAM ELEMENT, PROJECT, TASK AREA & WORK UNIT NUMBERS 121108
11. CONTROLLING OFFICE NAME AND ADDRESS Office of Naval Research Department of the Navy Arlington, VA 22217		12. REPORT DATE April 30, 1980
14. MONITORING AGENCY NAME & ADDRESS (if different from Controlling Office)		13. NUMBER OF PAGES 75
		15. SECURITY CLASS. (of this report)
		15a. DECLASSIFICATION/DOWNGRADING SCHEDULE
16. DISTRIBUTION STATEMENT (of this Report) Approved for public release; distribution unlimited.		
17. DISTRIBUTION ST. (Enter (if different from Report)		
18. SUPPLEMENTARY NOTES		
19. KEY WORDS (Continue on reverse side if necessary and identify by block number) Acoustic Imaging Nematic Acoustic Streaming		
20. ABSTRACT (Continue on reverse side if necessary and identify by block number) The program of this contract has been to study the acousto-optic effect which occurs in nematic liquid crystals when excited by acoustic waves, including extension and testing of the streaming model developed by C.F. Hayes. We have now for the first time developed and tested a mathematical model for proper cell design for this effect.		

Table of Contents

Introduction.....	1
Theory.....	3
Experiment:	
A. Single Laser Verification.....	16
B. Liquid Crystal Cell Investigation.....	19
Conclusions.....	26
References.....	27
Appendix A.....	28
Appendix B.....	32
Appendix C.....	41
Figures.....	50

I. INTRODUCTION

The acousto-optic effect is a phenomenon occurring in a nematic liquid crystal in the presence of both an ultrasonic wave and a linearly polarized light wave. The nematic cell is constructed by inserting the liquid crystal between two sheets of glass chemically treated to promote homeotropic alignment. Lecithin is a typical chemical agent which causes the long axes of the nematic molecules to become oriented perpendicular to the glass sheets. Normally no light is transmitted if the cell is observed between crossed polarizers. However, if an ultrasonic wave is directed to the cell, light will be transmitted through the second polarizer.

Since 1976 it has been known¹ that the mechanism causing the effect is acoustic streaming. However, the dependence of the effect upon the incident acoustic angle is not understood. In 1978, Letcher, Lebrun, and Candau² reported for their cells the effect took place in a relatively narrow range of incident angles, 27 to 30 degrees. In 1977, Nassi, Peters and Candau³ and, in 1978, Nassi and Iizuka⁴ reported the acoustic frequency dependence of the angular variation of sensitivity and gave preliminary results which indicated the transmitted light intensity increased with increased acoustic transmission. In 1979, Perbet, Harend, and LePerre⁵ reported strong light transmission at incident acoustic angles of maximum and minimum acoustic transmission. Also, in 1979, Lebrun, Candau, and Letcher⁶ reported the narrow angular range for the effect becomes broadened when thin glass is used for the cell.

In this report we describe the study we have undertaken to analyze the angular dependence of the acousto-optic effect. In Section II a theory is developed which gives the acoustic transmission of the cell as a function of incident acoustic angle, frequency, speed of the acoustic wave in the fluid(s) surrounding the cell, density of the cell, density of the fluid(s) surrounding the cell, density of the glass, speeds of the longitudinal and transverse waves in the glass, thickness of the glass layer, thickness of the liquid crystal and acoustic speed in the liquid crystal. Since each of these quantities are measurable, as well as the actual transmission, the final equation can be rigorously tested experimentally. The results of such testing is reported in Section III for both a single sheet of glass and the liquid crystal cell. A comparison is also made in this section between the acoustic transmission and sensitivity of the acousto-optic effect. This comparison gives insight into the results mentioned above by other researchers. We also obtain results for the angular dependence of lines which often appear in cells exhibiting the acousto-optic effect. In the final sections conclusions are drawn from these observations. Appendix A contains a computer program for evaluation of the acoustic transmission for a given set of the above mentioned parameters. Appendices B and C contain graphs of the transmission for typical cells as a function of angle for various frequencies.

II. THEORY

To obtain an expression for the transmission of an acoustic wave through a liquid crystal cell, we will use the coordinate system of Figure 1. Although experimentally we will immerse the cell in water the expression will allow the fluid on each side of the cell to be different.

Since fluids support no shear waves we will only have one wave function in the water and liquid crystal regions, a wave function for the compression wave:

$$\phi = (\phi' e^{i\alpha z} + \phi'' e^{-i\alpha z}) e^{i(\sigma x - \omega t)} \quad (1)$$

In the glass we will have an additional function for shear:

$$\psi = (\psi' e^{i\beta z} + \psi'' e^{-i\beta z}) e^{i(\sigma x - \omega t)} \quad (2)$$

We note that the x component of the wave number, σ , is the same for both types of waves. Due to Snell's Law we further see σ is the same in each medium.

The material speeds may be found from

$$v_x = \frac{\partial \phi}{\partial x} - \frac{\partial \psi}{\partial z} \quad (3)$$

and

$$v_x = \frac{\partial \phi}{\partial x} + \frac{\partial \psi}{\partial z} \quad (4)$$

The wave speeds may be expressed in terms of the Lame' parameters (λ, μ) and the density, ρ . The longitudinal speed is given by

$$c = \sqrt{\frac{\lambda + 2\mu}{\rho}} \quad (5)$$

and the shear speed by

$$b = \sqrt{\frac{\mu}{\rho}} \quad (6)$$

For the fluid region the only stress is the pressure, since $\mu = 0$, but for the glass regions we must generalize to

$$z_z = \lambda \left(\frac{\partial u_x}{\partial x} + \frac{\partial u_z}{\partial z} \right) + 2\mu \frac{\partial u_z}{\partial z} \quad (7)$$

$$z_x = \mu \left(\frac{\partial u_x}{\partial z} + \frac{\partial u_z}{\partial x} \right) \quad (8)$$

where u_x and u_z are material displacements from equilibrium in the x and z directions, respectively. These displacement components are related to the speed components by

$$u_x = \frac{iv}{\omega} x \quad (9)$$

$$u_z = \frac{iv}{\omega} z \quad (10)$$

As indicated in Figure 1 we use the subscript 1 to denote the water glass interface at $z=d$. We let

$$P = \alpha d = \omega d \cos \theta / c \text{ and } \theta = \beta d = d \cos \delta / b$$

Combining Equations 1 - 4 and 7 - 10 we have

$$\begin{pmatrix} v_{x_1} \\ v_{z_1} \\ z_{z_1} \\ \frac{1}{2} \mu z_{x_1} \end{pmatrix} = A \begin{pmatrix} \phi' + \phi'' \\ \phi' - \phi'' \\ \psi' - \psi'' \\ \psi' + \psi'' \end{pmatrix} \quad (11)$$

where

$$A = \begin{pmatrix}
 i\sigma \cos P & -\alpha \sin P \\
 -\alpha \sin P & i\alpha \cos P \\
 -\frac{i}{\omega} (\lambda k^2 + 2\mu\alpha^2) \cos P & \frac{1}{\omega} (\lambda k^2 + 2\mu\alpha^2) \sin P \\
 \frac{\alpha\sigma}{\omega} \sin P & -\frac{i\alpha\sigma}{\omega} \cos P \\
 \hline
 -i\beta \cos Q & \beta \sin Q \\
 -\sigma \sin Q & i\sigma \cos Q \\
 -\frac{2i\mu\sigma}{\omega} \beta \cos Q & \frac{2\mu\sigma\beta}{\omega} \sin Q \\
 \frac{1}{2\omega} (\sigma^2 - \beta^2) \sin Q & \frac{i(\beta^2 - \sigma^2)}{2\omega} \cos Q
 \end{pmatrix} \quad (12)$$

For interface 2 we write a similar equation:

$$\begin{pmatrix} v_{x_2} \\ v_{z_2} \\ z_{z_2} \\ \frac{1}{2\mu} z_{x_2} \end{pmatrix} = B \begin{pmatrix} \phi' + \phi'' \\ \phi' - \phi'' \\ \psi' - \psi'' \\ \psi' + \psi'' \end{pmatrix} \quad (13)$$

where B is obtained from A by letting $P=Q=0$. Of more interest is the inverse of B :

$$B^{-1} = \begin{pmatrix} \frac{-2i\sigma}{K^2} & 0 & \frac{i\omega}{\mu K^2} & 0 \\ 0 & \frac{-i(-\sigma^2 + \beta^2)}{\alpha K^2} & 0 & \frac{2i\omega}{\alpha K^2} \\ \frac{i(\lambda k^2 + 2\alpha^2 \mu)}{\beta \mu K^2} & 0 & \frac{i\omega}{\beta \mu K^2} & 0 \\ 0 & -2i\sigma/K^2 & 0 & \frac{-2i\omega}{K^2} \end{pmatrix} \quad (14)$$

We are using the notation of Brekhovskikh and Spielvogel. We take

$$k^2 = \sigma^2 + \alpha^2 \quad (15)$$

$$K^2 = \sigma^2 + \beta^2 \quad (16)$$

and use

$$\mu K^2 = k^2(2\mu + \lambda) \quad (17)$$

from Equations 5 and 6.

Combining Equations 11 and 13 we have

$$\begin{pmatrix} v_{x_1} \\ v_{z_1} \\ z_{z_1} \\ \frac{1}{2\mu} z_{x_1} \end{pmatrix} = A B^{-1} \begin{pmatrix} v_{x_2} \\ v_{z_2} \\ z_{z_2} \\ \frac{1}{2\mu} z_{x_2} \end{pmatrix} = a \begin{pmatrix} v_{x_2} \\ v_{z_2} \\ z_{z_2} \\ \frac{1}{2\mu} z_{x_2} \end{pmatrix} \quad (18)$$

We let $\sin \theta = \sigma/k$ and $\sin \gamma = \sigma/k$ so the components of a are

$$a_{11} = 2 \sin^2 \gamma \cos P + \cos 2\gamma \cos Q \quad (19)$$

$$a_{12} = i(\tan \theta \cos 2\gamma \sin P - \sin 2\gamma \sin Q) \quad (20)$$

$$a_{13} = \frac{\sin \theta}{\rho c} (\cos Q - \cos P) \quad (21)$$

$$a_{14} = -2ib(\tan \theta \sin \gamma \sin P + \sin Q \cos \gamma) \quad (22)$$

$$a_{21} = i \left[\frac{b \cos \theta \sin 2\gamma \sin P}{c \cos \gamma} - \tan \gamma \cos 2\gamma \sin Q \right] \quad (23)$$

$$a_{22} = \cos 2\gamma \cos P + 2 \sin^2 \gamma \cos Q \quad (24)$$

$$a_{23} = \frac{-i}{\rho c} (\cos \theta \sin P + \tan \gamma \sin \theta \sin Q) \quad (25)$$

$$a_{24} = 2b \sin \gamma (\cos Q - \cos P) \quad (26)$$

$$a_{31} = 2pb \sin \gamma \cos 2\gamma (\cos Q - \cos P) \quad (27)$$

$$a_{32} = -ip(c \frac{\cos^2 2\gamma}{\cos \theta} \sin P + 4b \cos \gamma \sin^2 \gamma \sin Q) \quad (28)$$

$$a_{33} = \cos 2\gamma \cos P + 2 \sin^2 \gamma \cos Q \quad (29)$$

$$a_{34} = 2i\rho b^2 (\cos 2\gamma \tan \theta \sin P - \sin 2\gamma \sin Q) \quad (30)$$

$$a_{41} = -i\left(\frac{2}{c} \cos \theta \sin^2 \gamma \sin P + \frac{\cos^2 2\gamma \sin Q}{2b \cos \gamma}\right) \quad (31)$$

$$a_{42} = \frac{\sin \theta \cos 2\gamma}{c} (\cos Q - \cos P) \quad (32)$$

$$a_{43} = \frac{i}{2\rho} \left(\frac{\sin 2\theta \sin P}{c^2} - \frac{\cos 2\gamma \tan \gamma \sin Q}{b^2} \right) \quad (33)$$

$$a_{44} = 2 \sin^2 \gamma \cos P + \cos 2\gamma \cos Q \quad (34)$$

The last component of Equation 18 is

$$\frac{1}{2\mu} z_{x_1} = a_{41} v_{x_2} + a_{42} v_{z_2} + a_{43} z_{z_2} + a_{44} z_{x_2} / 2\mu \quad (35)$$

This equation describes what happens at the glass fluid interface. However, since there can be no transverse stress in the fluid we must also have no transverse stress in the glass at the boundary: $z_{x_1} = z_{x_2} = 0$. Therefore Equation 35 reduces to

$$a_{41} v_{x_2} + a_{42} v_{z_2} + a_{43} z_{z_2} = 0 \quad (36)$$

Incorporating Equation 36 into Equation 18 we obtain

$$v_{x_1} = \left(a_{12} - \frac{a_{11} a_{42}}{a_{41}} \right) v_{z_2} + \left(a_{13} - \frac{a_{11} a_{43}}{a_{41}} \right) z_{z_2} \quad (37)$$

$$\begin{pmatrix} v_{z_1} \\ z_{z_1} \end{pmatrix} = \begin{pmatrix} M_1 & M_2 \\ M_3 & M_4 \end{pmatrix} \begin{pmatrix} v_{z_2} \\ z_{z_2} \end{pmatrix} \quad (38)$$

where

$$M_1 = a_{22} - a_{21} a_{42} / a_{41} \quad (39)$$

$$M_2 = a_{23} - a_{21} a_{43} / a_{41} \quad (40)$$

$$M_3 = a_{32} - a_{31} a_{42} / a_{41} \quad (41)$$

$$M_4 = a_{33} - a_{31} a_{43} / a_{41} \quad (42)$$

In a fluid $b=0$ and $\delta=0$ so to relate v_z and z_z between interfaces 2 and 3 we have analogous to Equation 38:

$$\begin{pmatrix} v_{z_2} \\ z_{z_2} \end{pmatrix} = \begin{pmatrix} a_{22} & a_{23} \\ a_{32} & a_{33} \end{pmatrix} \begin{pmatrix} v_{z_3} \\ z_{z_3} \end{pmatrix} \quad (43)$$

where

$$a_{22}' = \cos P_{LC} \quad (44)$$

$$a_{23}' = \frac{-i \sin P_{LC} \cos \theta_{LC}}{\rho_{LC} C_{LC}} \quad (45)$$

$$a_{32}' = \frac{-i \rho_{LC} C_{LC} \sin P_{LC}}{\cos \theta_{LC}} \quad (46)$$

$$a_{33}' = \cos P_{LC} \quad (47)$$

where the LC subscript refers to the value of these parameters in the liquid crystal region.

We have for the second glass region:

$$\begin{pmatrix} v_{z_3} \\ z_{z_3} \end{pmatrix} = \begin{pmatrix} M_1 & M_2 \\ M_3 & M_4 \end{pmatrix} \begin{pmatrix} v_{z_4} \\ z_{z_4} \end{pmatrix} \quad (48)$$

where the M_i 's are given in Equations 39-42.

Equations 38, 43, and 48 combine to give

$$\begin{pmatrix} v_{z_1} \\ z_{z_1} \end{pmatrix} = \begin{pmatrix} C_1 & C_2 \\ C_3 & C_4 \end{pmatrix} \begin{pmatrix} v_{z_4} \\ z_{z_4} \end{pmatrix} \quad (49)$$

where

$$\begin{pmatrix} C_1 & C_2 \\ C_3 & C_4 \end{pmatrix} = \begin{pmatrix} M_1 & M_2 \\ M_3 & M_4 \end{pmatrix} \begin{pmatrix} a_{22}' & a_{23}' \\ a_{32}' & a_{33}' \end{pmatrix} \begin{pmatrix} M_1 & M_2 \\ M_3 & M_4 \end{pmatrix} \quad (50)$$

Equation 49 relates the z component of stress and velocity of interface 1, the first interface the incident wave encounters, to interface 4, the final interface of the cell. We may now match the incident wave with interface 1 and the transmitted wave with interface 4 and thereby find the acoustic transmission of the cell. We will change the origin of the coordinate system in Figure 1 so it lies in interface 4 and take the complete cell thickness from 1 to 4 to be H . Then for the initial wave we have

$$\phi_a = [\phi_a' e^{i\alpha_a(z-H)} + \phi_a'' e^{-i\alpha_a(z-H)}] e^{i(\sigma_a x - \omega t)} \quad (51)$$

$$\psi_a = 0 \quad (52)$$

where ϕ'' is the amplitude of the incident wave and ϕ' the amplitude of the reflected wave. The wave is traveling in the negative z direction.

Similarly for fluid b

$$\phi_b = \phi_b' e^{-i\alpha_b z} e^{i(\sigma_b x - \omega t)} \quad (53)$$

for the wave transmitted through the cell. Using Equations 3, 4, and 7-10 and omitting the common factor of $e^{i(\sigma x - \omega t)}$ we have

$$v_{xa} = i\sigma_a (\phi_a' + \phi_a'') \quad (54)$$

$$v_{za} = i\alpha_a (\phi'_a - \phi''_a) \quad (55)$$

$$z_{xa} \approx 0 \quad (56)$$

$$z_{za} = -i\omega p_a (\phi'_a + \phi''_a) \quad (57)$$

$$v_{xb} = i\alpha_b \phi'''_b \quad (58)$$

$$v_{zb} = -i\alpha_b \phi'''_b \quad (59)$$

$$z_{zb} = -i\omega p_b \phi'''_b \quad (60)$$

From Equation 49 we have

$$\begin{pmatrix} -\alpha_a (\phi'_a - \phi''_a) \\ \omega p_a (\phi'_a + \phi''_a) \end{pmatrix} = \begin{pmatrix} c_1 & c_2 \\ c_3 & c_4 \end{pmatrix} \begin{pmatrix} \alpha_b & \phi'''_b \\ \omega p_b & \phi'''_b \end{pmatrix} \quad (61)$$

We define the transmission coefficient as

$$D = \rho_b \phi'''_b / \rho_a \phi'''_a \quad (62)$$

and the reflection coefficient as

$$V = \phi'_a / \phi''_a \quad (63)$$

Equation 61 provides the means by which these coefficients may be evaluated. To calculate the transmitted acoustic intensity we must evaluate (61). Care must be taken in doing so, however. The longitudinal speed in the glass is over three times the speed in the water. Use of Snell's law shows the critical angle for the two types of glass we use occurs at 15 degrees and 15.5 degrees. Similarly, the shear wave speed in the glass is over twice the longitudinal speed in the water. For the two types of glass we use the critical angle for this type of wave is exceeded at 25.5 and 27 degrees. Therefore, we find three regions for the angle of incidence. A separate equation for the transmission must be found for each region: the region where no critical angle is exceeded, where only the critical angle for the longitudinal wave is exceeded and where both critical angles are exceeded. For example, in the second region taking Θ to be the angle for the compression wave in the glass and Θ_a in the water we have from Snell's law

$$\frac{\sin \theta}{C_a} = \frac{C \sin \theta_a}{C_a} \quad \text{so if } \frac{C \sin \theta_a}{C_a} > 1 \text{ then}$$

$$\cos \theta + i \sqrt{\sin^2 \theta - 1} \quad (64)$$

$$\sin P + i \sinh |P| \quad (65)$$

$$\cos P + \cosh |P| \quad (66)$$

Similarly, if both critical angles are exceeded we must make changes in $\cos \chi$, $\sin Q$, and $\cos Q$.

Therefore certain terms which are real in the matrices for one region will be imaginary in another. Nevertheless we do find for all regions :

$$|D|^2 = \frac{4\omega^2 \rho_b^2 / \alpha_b^2}{\left[\frac{\omega \rho_b}{\alpha_b} |C_4| + \frac{\omega \rho_a}{\alpha_a} |C_1| \right]^2 + \left[|C_3| + \frac{\omega^2 \rho_a \rho_b}{\alpha_a \alpha_b} |C_2| \right]^2} \quad (67)$$

although the form for $|C_i|$ will change for each region.

Equation 67 will be the basis of comparison for the measurements we will make for the amount of ultrasound transmitted through the liquid crystal cell. It should be noted that Equation 67 does not include any damping due to either viscosity or surface waves in the cell. Furthermore, we have omitted the small anisotropy for the speed of sound which occurs in liquid crystals. The latter simplification appears to be less severe than the former ones.

III EXPERIMENT

A. Single Laser Verification

To test Equat. 167 experimentally, we start with the simple case of a single sheet of glass rather than the liquid crystal cell mentioned above. For this case the $1C_1$ reduce to the $1M_1$ of Equations 39 - 42.

Two Panometrics Model V302 transducers are used for the transmitter and hydrophone. The transmitter is driven by a Hewlett-Packard Model 3312A function generator in the amplitude-modulation mode externally modulated by a Hewlett-Packard Model 3310A pulse generator. Pulses were typically 25 μ sec in width containing approximately 20 cycles per pulse. The frequency is measured using a Hewlett-Packard Model 5326A timer/counter. The glass sheet is placed in the center of a water tank 30cm x 40cm x 60cm. The acoustic transmitter is located 8 cm from the glass sheet with the hydrophone approximately the same distance on the other side. The glass is suspended by an angular positioning device allowing orientation to the nearest degree to be specified. Initial alignment is facilitated by a laser. The signal from the hydrophone is amplified and sent to both a PAR Model 160 boxcar integrator and Tektronix 564 oscilloscope. For the data on the graphs presented in this section the values are read from the oscilloscope.

The glass sheets are 15 cm x 15 cm x 0.16 cm and 15 cm x 15 cm x 0.0146 cm, respectively. The diameter of both the transmitter and hydrophone are 2.5 cm. By noting the time of the various pulses

displayed on the oscilloscope the reflection source may be identified, as the orientation of the glass changes the times between the reflection pulses and main pulse changes. The largest reflected pulse amounts to 10% of the main pulse.

The following constants are used for the thicker glass, longitudinal and shear speeds: 5.61×10^5 cm/sec and 3.32×10^5 cm/sec, respectively, with a density of 2.54 gm/cm^3 . For the thin glass these values are 5.81×10^5 cm/sec, 3.48×10^5 cm/sec and 2.51 gm/cm^3 , respectively. The thicker glass is float glass obtained from PPG Industries. The manufacturer supplied the values of Young's modulus, $1.0 \times 10^7 \text{ lb/in}^2$, and the Poisson ratio, 0.23, from which the above acoustic speeds are obtained. The thin glass is obtained from Corning Glass Co. which supplied the shear modulus, $4.4 \times 10^6 \text{ psi}$, and Poisson ratio, 0.22, from which the acoustic speeds for the thin glass are calculated.

Figure 2 is a graph of the ratio of the hydrophone voltage with the glass present to that without. The abscissa is the angle between the normal to the glass plate and that of the acoustic beam. The crosses are the experimental values obtained approximately every degree. The solid line is the theoretical result from Equation 67 for IDI using the above constants. It should be noted that there are no adjustable parameters used in this graph since each constant of Equation 67 is known. There are two peaks of 100% transmission in the theoretical plot at 16.5 degrees and ~ 35.4 degrees, as well as a dip to zero transmission at 15.9 degrees. Experimentally the crosses in the graph show the upper peak, though shifted to 34.5 degrees and

reduced from 100% to 70% transmission. The lower peak and dip are missing, however. These discrepancies are due in part to the finite acceptance angle of the hydrophone. Figure 3 is identical to Figure 2 except each point on the theoretical plot is averaged over the values for 3 degrees on each side. The averaging brings the upper peak down to a maximum of 82.9% and places it at 35.2 degrees as well as greatly reducing the lower peak and almost eliminating the dip. This averaging will be performed in the subsequent graphs.

Figure 4 shows the comparison of theory and experiment for a single sheet of the thin glass. The theory appears to uniformly predict two to three percent higher transmission than what is realized experimentally, in agreement with Figure 3. Considering we have omitted any dissipation of the sound wave we would expect such a result. A frequency of 0.858 MHz is used for Figures 2 and 3 and 0.857 MHz for Figure 4. For the thicker glass the resulting wavelengths for the longitudinal and shear waves are, respectively, 0.65 cm and 0.39 cm. The ratio of wavelength to glass thickness is 0.25 and 0.41, respectively. For the thinner glass the longitudinal and shear wavelengths are 0.021 and 0.036, respectively. It is this smaller ratio for the thin glass which makes it suited for the nematic cell exhibiting the acousto-optic effect. We shall see the uniform higher sound transmission allows for a greater light transmission in the acousto-optic effect with less angular sensitivity.

B. Liquid Crystal Cell Investigation

The nematic liquid crystal is 4 - cyan - 4' - n hexyl biphenyl commonly known as K18. The transition temperature for the crystal to nematic phase transition occurs at 14.5° C and the nematic to isotropic transition at 29.4° C. It is obtained from Atomergic Chemicals Corp. and used without further purification.

Each cell is constructed by coating two glass sheets with lecithin to promote homeotropic alignment of the liquid crystal. The coated sides are placed next to one another with 80 μ m spacers at the edges. The liquid crystal is then introduced at the glass edges between the spacers and pulled into the cell by capillary action.

After the cell has been filled with the nematic the edges are coated with wax. Epoxy is then applied at all edges. The wax is used to prevent the nematic from reacting chemically with the epoxy. For cells made with the thin glass the cell is mounted in a plexiglass frame for added support.

The acoustic wave for these cells is generated by the method described above or with a Medi-Sonar Model 1100 ultrasonic generator. The latter operates at 1 MHz and is used when greater power is required. Intensities of 1.1 Watts/ cm^2 may be obtained with this unit.

For measurement of the light transmitted by the acousto-optic effect a 150 Watt lamp is used. Light passes through the liquid

crystal cell, a second polarizer with an axis oriented at 90 degrees to the first, and to a photomultiplier. The signal from the photomultiplier is amplified and sent to a digital voltmeter.

Figure 5 shows the ratio of voltage to the hydrophone, with and without the liquid crystal cell, as a function of angle. For Figure 5 the cell is constructed of the thicker glass and an acoustic frequency of 1 MHz is used. The crosses are the experimental ratios and the solid line is the theoretical value of TB/I from Equation 67. The details of the program used for the evaluation of Equation 67 is found in Appendix A. The solid points on the graph are for the light intensity in arbitrary units transmitted via the acousto-optic effect.

It would appear the acousto-optic effect is operative when the cell configuration allows maximum transmission of sound. This result appears to explain the results of Letcher, Lebrun and Candau² who reported a strong optical signal for only a narrow range of incident angles, 27 to 30 degrees. This result is also in agreement with Nassi, Peters and Candau³ who found a correlation with experimental acoustic and optical transmission. Equation 67 also explains their results for acoustic transmission versus film thickness, their Figure 7. Also, the broadening of the transmission for thin glass as reported by Lebrun, Candau and Letcher² is explained. This result is in disagreement to that of Perbet, Harens and LeBerre⁵ who report an optical signal for large acoustic reflection. We find no optical signal for large acoustic reflection.

If we conclude that Equation 67 may be used to predict maximum acoustic transmission and therefore maximum transmitted light from the acousto-optic effect it would appear the equation could be used to prescribe how a given cell should be made for a particular acoustic frequency. Or if the cell size is determined by other considerations, Equation 67 could be used to prescribe the acoustic frequency which should be used. For instance, for the thicker glass cell used in Figure 5, assuming an incident angle of zero, Equation 67 is used to determine the acoustic transmission. See Figure 6. The results indicate that an acoustic frequency of around 500 kHz would give the best results.

For Figure 7 the cell was constructed of the thinner glass sheets. Again we see as the acoustic transmission increases more light is transmitted. In comparing Figure 7 with Figure 4 and Figure 5 with Figure 3 we see the difference in the theoretical sound transmission and experimental sound transmission increases as one changes from a single glass sheet to a liquid crystal cell. The increase is reasonable since the means of dissipation has increased. The flows induced in the liquid crystal which give rise to the acousto-optic effect are in fact an added means of dissipation of the acoustic energy.

Another means of dissipation is the surface wave generated. Figure 8 shows a series of photographs for the cell viewed between crossed polarizers. The photographs labeled A to F have the incident acoustic beam at angles 0° , 4° , 12.5° , 15° , -17° (from the right rather than the left), and 33° . The dark circle with the knob on the left in

the photographs is the acoustic transmitter. The small tilted rectangle in each picture is a spacer. In each picture vertical lines are shown. In the absence of acoustic waves these lines disappear. The light transmitted in each line is the result of acoustic streaming in the liquid crystal (i.e. the acousto-optic effect). As the angle of incidence increases the distance between the lines decreases. Figure 9 is a graph of the line spacing as a function of angle. If we imagine a plane wave of incident angle, θ , coming to the cell surface the component, d , of the wavelength along the surface is given by

$$d = \frac{\lambda}{\sin\theta} \quad (68)$$

We would expect a surface wave to be generated and the distance between the lines to be proportional to d . Since for normal incidence Equation (68) shows d to become infinite we generalize the equation to

$$\text{line spacing} = a/\sin(\theta + b) \quad (69)$$

where a and b are constants. The constant b should result from the divergence of the incident acoustic beam. The continuous curve in Figure 9 is for Equation 69 with $a=1.25$ mm and $b=14.38$ degrees. Lines similar to these have been reported by Perbet, Harens, and LeBerre.⁵ The angular dependence we observe lends support to their claim that the lines result from surface waves.

From Equations 38, 43, 48, 59, and 60 we find the ratio of v_{22}

to v_{23}

$$\frac{v_2}{v_3} = \frac{A_1 + A_2 \left[M_3 + \frac{\rho_b C_b M_4}{\cos \theta_b} \right]}{\left[M_1 + \frac{\rho_b C_b M_2}{\cos \theta_b} \right]} \quad (70)$$

Since this ratio is complex it contains information concerning the phase. The two surfaces, labeled 2 and 3, are the liquid crystal boundaries. If this phase is 180 degrees we have a peristaltic wave traveling along the liquid crystal layer. If the phase is zero degrees we have an ordinary flexural wave. In Figures 10 and 11 the phase calculated from Equation 70 is plotted as a function of incident acoustic angle for the thick glass and the thin glass cells respectively. Referring to Figure 5 we see there is a significant amount of light from the acousto-optic effect for incident angles in the range of 29 to 33 degrees. From Figure 10 we see the boundaries are out of phase (50 to 140 degrees) in this region giving rise mainly to a peristaltic wave. From Figure 7 we find for the thin glass cell the light intensity increases with angle and from Figure 11 the phase difference becomes smaller with angle to a phase of around 20 degrees at an incident angle of 40 degrees generating mainly a flexural wave. It would appear therefore the important feature giving rise to the acousto-optic effect is the amplitude of vibration for the liquid crystal boundaries as indicated above rather than the relative phase.

It is of interest therefore to see how the angular transmission

changes as a function of the acoustic frequency for the cells. Appendix B is a series of graphs which show the theoretical value of $|\Gamma|$ from Equation 67 as a function of angle for the thick glass cell. For low frequencies, 100 kHz, for which the ratio of acoustic wavelength to thickness of a single glass plate is about 0.03 the curve is fairly flat with a transmission greater than 50% for all angles less than 60 degrees. As the frequency is increased to 300 kHz the lower angle transmission decreases and a peak appears at higher angles. The peak becomes narrower at 400 kHz and appears at a lower angle. By 500 kHz a peak has appeared at lower angles, as well, and is seen to increase in location at 600 kHz. These peaks continue to approach one another and are nearly superimposed at one MHz.

In Appendix C a series for a thin glass cell is presented. For the first graph the frequency is 1.0 MHz which still gives an acoustic wavelength to glass thickness of about 0.03 since the glass is so thin. Again we see a rather flat curve with the transmission above 60% for all angles. At 2 MHz a peak appears and at 3 MHz a second one. At 4 MHz the two peaks have narrowed and merged. The narrowing continues to 8 MHz.

In Figure 12 the theoretical plot of amplitude ratio versus the thickness of the nematic layer is plotted for an acoustic frequency of 1 MHz and zero acoustic incident angle. It would appear from the sound transmission the best thickness for a cell made of the thin glass would occur at 200 micrometers. For higher frequencies the peak occurs at lower thicknesses and is narrower. At 1.9 MHz the peak occurs at 70 micrometers.

In Figure 13 the theoretical amplitude is given as a function of acoustic frequency, for a cell of the thin glass with zero acoustic incident angle. The decrease in ratio above 3 MHz continues up through 8 MHz, as seen in Appendix C. It would appear the best frequency occurs at 1.9 MHz. Therefore, we conclude the best cell for the thin glass and for zero incident acoustic angle would occur for a frequency of 1.9 MHz and find the optimum nematic thickness to be 70 micrometers.

IV. CONCLUSIONS

We have developed an equation to allow evaluation of the acoustic transmission through a liquid crystal cell as a function of incident acoustic angle, frequency and thickness, density and acoustic speeds of the materials in the cell. Although a number of simplifying assumptions are made in the derivation, such as omitting viscous dissipation, we find good agreement between the theoretical prediction and the experimental realization for acoustic transmission. We also find a positive correlation between the maximum acoustic transmission and the maximum sensitivity for the acousto-optic effect. Therefore, the transmission equation may be used to prescribe cell structure and acoustic frequency for the utilization of the acousto-optic effect. Appendices B and C contain examples of how one may use the equation in this way. The maximum acoustic transmission of the cell occurs at those angles where the component of the incident wavelength along the glass surface matches the wavelength of a flexural or peristaltic wave along the glass at the imposed acoustic frequency. Therefore, the maximum acoustic transmission occurs when the liquid crystal boundaries have their largest amplitudes of oscillation. The result is important for the resolution of a visualized acoustic wavefront pattern. To increase the resolution we must not only dampen the lateral flow of the liquid crystal but we must dampen the lateral flexural or peristaltic wave induced in the glass walls. There are several means of inducing such damping. We are presently attempting to increase the cell resolution by increasing the lateral damping.

REFERENCES

1. C. Sripraman, C.F.Hayes and G.T.Fang, Sixth International Liquid Crystal Conference, J-29 (1976).
C. Sripraman, C.F.Hayes and G.T.Fang, Phys. Rev. 15A, 1297 (1977).
K. Miyano and Y.R.Shen, Appl.Phys.Lett. 28, 473 (1976).
2. S.Letcher, J.Lebrun and S.Candau, J.Acoust.Soc.Am. 63, 55 (1978).
3. S.Nasai, A.Peters and S. Candau, Revue Phys.Appl. 12, 21 (1977).
4. S.Nasai and K.Iizuka, Japan.J.Appl.Phys. 17, 723 (1978).
5. J.N.Perbet, M.Harens and S.LeBerre, Rev.Phys.Appl. 14, 569 (1979).
6. J.Lebrun, S.Candau, S.V. Letcher, Jour. Phys. C3, 298 (1979).
7. L.M.Brekhovskikh, Waves in Layered Media (Academic, New York, 1960), pp. 56 ff.
8. L.Q.Spielvogel, Jour.Appl.Phys. 42, 3667 (1971).

APPENDIX A

Appendix A contains a program in Basic to give the acoustic transmission through a liquid crystal cell as a function of incident acoustic angle.

```

10 V1=0
20 REM DENSITY R1(H20), R(GLASS), R3(L.C.), R4(AIR OR H20)
30 REM SPEED C1(H20), C(GLASS), B(GLASS), C3(L.C.), C4(AIR OR)
40 REM DISTANCE D1(L.C.), D2(GLASS)
50 REM ANGLE V1(H20) = THE INITIAL ANGLE
160 R3=1
170 R4=1
180 R1=1
190 C4=150000
200 F=900000
210 R=2.54
220 C1=150000
230 C=560845
240 B=332216
250 C3=150000
260 D1=.008
270 D2=.0146
300 IF C*SIN(V1)/C1>1 THEN 400
310 GOTO 1000
400 IF B*SIN(V1)/C1>1 THEN 5000
410 GOTO 3000
1000 S8=C*SIN(V1)/C1
1010 S9=B*SIN(V1)/C1
1020 C8=SQRT(1-1*S8^2)
1030 C9=SQRT(1-1*S9^2)
1040 C7=2*C9^2-1
1050 F=2*3.14159*F*D2*C8/C
1070 Q=2*3.14159*F*D2*C9/B
1080 S6=SIN(P)
1090 C6=COS(P)
1100 S5=SIN(Q)
1110 C5=COS(Q)
1120 J1=2*B*C8*S6*S9/C-S9*C7*S5/C9
1130 J2=C7*C6+2*S9^2*C5
1140 J3=-S8*S9*S5/(C*R*C9)-C8*S6/(C*R)
1150 K1=-2*B*R*S9*C7*C6+2*B*R*S9*C7*C5
1160 K2=-4*B*R*S9^2*C9*S5-C*R*C7^2*S6/C8
1170 K3=C7*C6+2*S9^2*C5
1180 L1=-1*C7^2*S5/(2*B*C9)-2*S9^2*C8*S6/C
1190 L2=-S8*C7*C6/C+S8*C7*C5/C
2000 L3=-S9*C7*S5/(2*B^2*R*C9)+S6*S8*C8/(C^2*R)

```

```

2010 M1=J2-J1*L2/L1
2020 M2=J3-J1*L3/L1
2030 M3=K2+K1*L2/L1
2040 M4=K3-K1*L3/L1
2050 T8=C3*SIN(V1)/C1
2060 U8=SQRT(1-T8^2)
2070 P1=2*3.14159*F*D1*U8/C3
2080 A1=COS(P1)
2090 A2=-SIN(P1)*U8/(R3*C3)
2100 A3=-R3*C3*SIN(P1)/U8
2110 A4=A1
2120 E1=-M1*M2*A3-M1*M3*A2-M2*M3*A4+M1*M1*A1
2130 E2=M1*M2*A1+M1*M4*A2+M2*M4*A4-M2*M2*A3
2140 E3=M1*M3*A1+M1*M4*A3+M3*M4*A4-M3*M3*A2
2150 E4=-M2*M3*A1-M2*M4*A3-M3*M4*A2+M4*M4*A4
2160 Z1=R1*C1/COS(V1)
2170 Z4=R4*C4/SQRT(1-1*(C4*SIN(V1)/C1)^2)
2180 T2=4*Z4^2/((Z4*E4+Z1*E1)^2+(E3+Z1*Z4*E2)^2)
2189 T2=SQRT(T2)
2190 PRINT INT(10*V1*180/3.14)/10,T2,TAB(15+50*T2), "*"
2200 V1=V1+3.14159/180
2210 IF V1>70*3.14/180 THEN 8000
2220 GOTO 300
3000 S8=C*SIN(V1)/C1
3010 S9=B*SIN(V1)/C1
3020 C8=SQRT(S8^2-1)
3030 C9=SQRT(1-1*S9^2)
3040 C7=2*C9^2-1
3050 P=2*3.14159*F*D2*C8/C
3060 Q=2*3.14159*F*D2*C9/B
3070 S6=(EXP(P)-EXP(-P))/2
3080 C6=(EXP(P)+EXP(-P))/2
3084 S5=SIN(Q)
3085 C5=COS(Q)
3090 J1=-B*C8*S6*2*S9/C-S9*C7*S5/C9
3100 J2=C7*C6+2*S9^2*C5
3110 J3=-S8*S9*S5/(C*R*C9)+C8*S6/(C*R)
3120 K1=-2*B*R*S9*C7*C6+2*B*R*S9*C7*C5
3130 K2=-4*B*R*S9^2*C9*S5-C*R*C7^2*S6/C8
3140 K3=C7*C6+2*S9^2*C5
3150 L1=-1*C7^2*S5/(2*B*C9)+2*S9^2*C8*S6/C
3160 L2=-S8*C7*C6/C+S8*C7*C5/C
3170 L3=-S9*C7*S5/(2*R^2*R*C9)-S6*S8*C8/(C^2*R)
3180 GOTO 2010

```

```
5000 S8=C*SIN(V1)/C1
5010 S9=B*SIN(V1)/C1
5020 C8=SQRT(S8^2-1)
5030 C9=SQRT(S9^2-1)
5040 C7=-2*C9^2-1
5050 P=2*3.14159*F*I2*C8/C
5060 Q=2*3.14159*F*I2*C9/B
5070 S6=(EXP(P)-EXP(-P))/2
5080 C6=(EXP(P)+EXP(-P))/2
5090 S5=(EXP(Q)-EXP(-Q))/2
5100 C5=(EXP(Q)+EXP(-Q))/2
5110 J1=-B*C8*S6*2*S9/C-S9*C7*S5/C9
5120 J2=C7*C6+2*S9^2*C5
5130 J3=-S8*S9*S5/(C*R*C9)+C8*S6/(C*R)
5140 K1=-2*B*R*S9*C7*C6+2*B*R*S9*C7*C5
5150 K2=4*B*R*S9^2*C9*S5-C*R*C7^2*S6/C8
5160 K3=C7*C6+2*S9^2*C5
5170 L1=-1*C7^2*S5/(2*B*C9)+2*S9^2*C8*S6/C
5180 L2=-S8*C7*C6/C+S8*C7*C5/C
5190 L3=-S9*C7*S5/(2*B^2*R*C9)-S6*S8*C8/(C^2*R)
5200 OOTD 2010
8000 END
```

APPENDIX B

Appendix B contains the computer print-out for the acoustic transmission as a function of angle for a liquid crystal cell using glass 1.6 mm thick and a liquid crystal layer 0.08 mm thick. The frequencies used vary from 100 kHz to 1 MHz.

RUN

FREQUENCY = 100000
ANGLE SQ.ROOT T2

0	.53031519
2	.53049074
4	.53101764
6	.5318928
8	.53310191
10	.53458961
12	.53614786
14	.53671979
16	.50364879
18	.55621914
20	.55744664
22	.56194362
24	.5678085
26	.57475542
28	.58273586
30	.59176335
32	.60187158
34	.61309946
36	.62548237
38	.63904676
40	.65380648
42	.66976124
44	.68688188
46	.70511943
48	.7243843
50	.74456355
52	.7654945
54	.7869849
56	.80879108
58	.83065597

FREQUENCY = 200000
ANGLE SQ.ROOT T2

0	.34651734	*
2	.34652966	*
4	.34656605	*
6	.34661781	*
8	.34664528	*
10	.34650293	*
12	.34565976	*
14	.34146675	*
16	.26142596	*
18	.3775428	*
20	.37185371	*
22	.37389204	*
24	.37855749	*
26	.38512721	*
28	.39352561	*
30	.40387373	*
32	.41638878	*
34	.43135173	*
36	.44909745	*
38	.47001909	*
40	.49453893	*
42	.52311694	*
44	.55619384	*
46	.59413948	*
48	.63713051	*
50	.68497456	*
52	.73683352	*
54	.79120591	*
56	.84526676	*
58	.89552709	*

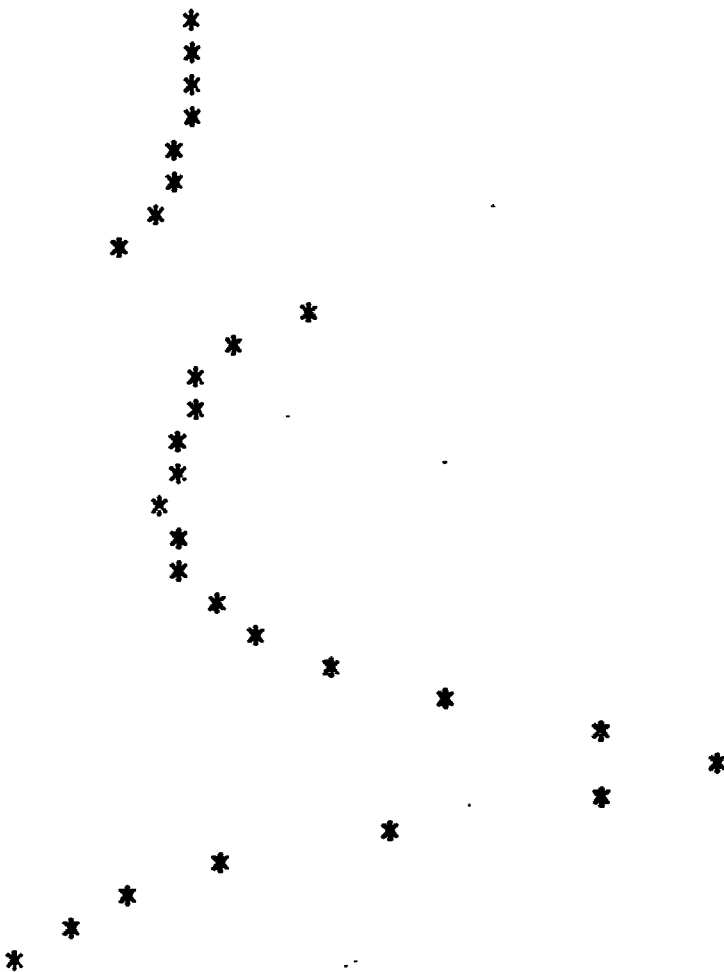
FREQUENCY = 300000

ANGLE SQ.ROOT T2

0	.32365379	*
2	.32349096	*
4	.32298899	*
6	.32209405	*
8	.32066008	*
10	.31828903	*
12	.31372772	*
14	.30122937	*
16	.15743477	*
18	.37393455	*
20	.35301396	*
22	.349408	*
24	.35052289	*
26	.35454088	*
28	.36123751	*
30	.37090848	*
32	.38415687	*
34	.40186889	*
36	.4252746	*
38	.45605482	*
40	.49648752	*
42	.54959309	*
44	.61903527	*
46	.70804023	*
48	.81524999	*
50	.92433679	*
52	.99392697	*
54	.98251658	*
56	.90117879	*
58	.79729963	*

FREQUENCY = 400000
ANGLE SQ.ROOT T2

0 .44575546
2 .44550411
4 .4446042
6 .44258774
8 .43854122
10 .43071006
12 .41496347
14 .37567037
16 9.9410913E-02 *
18 .57428437
20 .49033762
22 .45981837
24 .44093094
26 .42797399
28 .42019843
30 .41826343
32 .42357769
34 .43836952
36 .4661941
38 .51296621
40 .58873302
42 .7088387
44 .87912815
46 .99979624
48 .87226826
50 .64427637
52 .47698099
54 .37026756
56 .30125195
58 .25502811



FREQUENCY = 500000
ANGLE SQ.ROOT T2

0 .9975715
2 .99701681
4 .99530841
6 .99285562
8 .99154948
10 .99454156
12 .99999471
14 .94080152
16 6.2643351E-02 *

18 .86642261
20 .99819855
22 .9556492
24 .83643918
26 .71178303
28 .61440708
30 .54968327
32 .51535038
34 .51080818
36 .54167181
38 .62599924
40 .80105178
42 .99890843
44 .75957952
46 .45576596
48 .296223
50 .21062089
52 .16009318
54 .12793822
56 .10637034
58 .09137821

*

*

*

*

*

*

*

*

*

*

*

*

*

*

*

*

*

*

*

*

*

*

*

*

*

*

*

*

*

*

*

*

*

*

FREQUENCY = 600000
ANGLE SQ.ROOT T2

0	.30500073	*
2	.30179229	*
4	.29326018	*
6	.28215715	*
8	.2718099	*
10	.26538554	*
12	.26626798	*
14	.28324073	*
16	3.8622229E-02*	
18	.30400601	*
20	.36175208	*
22	.46167116	*
24	.63904649	*
26	.90453746	
28	.97731108	
30	.78256852	*
32	.6412908	
34	.59504245	*
36	.64279457	*
38	.83487877	*
40	.95840298	*
42	.50310603	*
44	.26612626	*
46	.16407183	*
48	.11207212	*
50	8.2105742E-02 *	
52	6.3350093E-02 *	
54	5.0914309E-02*	
56	4.2331909E-02*	
58	3.6242261E-02*	

FREQUENCY = 800000

ANGLE SQ.ROOT T2

0	.09482626	*
2	.9.2695369E-02	*
4	8.7360146E-02	*
6	8.1001516E-02	*
8	7.5340103E-02	*
10	7.1025114E-02	*
12	6.7548982E-02	*
14	6.1327748E-02	*
16	5.2167358E-04*	
18	.12910011	*
20	.12714057	*
22	.14878961	*
24	.19321683	*
26	.28436823	*
28	.50303717	*
30	.95537299	
32	.84255748	*
34	.75271136	*
36	.99470917	*
38	.44571181	*
40	.16920712	*
42	.08498257	*
44	4.9745958E-02*	
46	3.2026262E-02*	
48	2.2039981E-02*	
50	1.5959212E-02*	
52	1.2043273E-02*	
54	9.4132979E-03*	
56	.00758951	*
58	6.2938972E-03*	

FREQUENCY = 700000

ANGLE SQ.ROOT T2

0	.14614023	*
2	.14398759	*
4	.13834244	*
6	.1310977	*
8	.12417377	*
10	.11882437	*
12	.11532526	*
14	.1114234	*
16	3.6084021E-02*	
18	.17296716	*
20	.18446955	*
22	.22275625	*
24	.29682343	*
26	.4481302	*
28	.77005966	
30	.98714771	*
32	.76241145	
34	.67384193	*
36	.79491955	
38	.95902435	*
40	.41070682	*
42	.19101633	*
44	.10856379	*
46	6.9545699E-02 *	
48	.04819727	*
50	3.5364793E-02*	
52	.02713297	*
54	2.1596886E-02*	
56	1.7743446E-02*	
58	.01499378	*

RUN

FREQUENCY = 1000000
ANGLE SQ.ROOT T2

0 .062	*
2 .054	*
4 .044	*
6 .039	*
8 .037	*
10 .035	*
12 .034	*
14 .027	*
16 .012	*
18 .119	*
20 .097	*
22 .107	*
24 .133	*
26 .188	*
28 .331	*
30 .795	*
32 .895	*
34 .992	*
36 .312	*
38 .094	*
40 .04	*
42 .021	*
44 .012	*
46 .007	*
48 .004	*
50 .003	*
52 .002	*
54 .001	*
56 .001	*
58 .001	*

APPENDIX C

Appendix C contains the computer print-out for the acoustic transmission as a function of angle for a liquid crystal cell using glass 0.146 mm thick and a liquid crystal layer 0.08 mm thick. The frequencies used vary from 1 MHz to 8 MHz.

RUN

FREQUENCY = 1000000

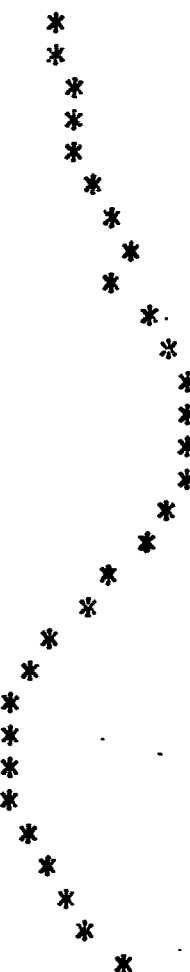
ANGLE SQ.ROOT T2

0 .697
2 .697
4 .697
6 .697
8 .697
10 .697
12 .697
14 .694
16 .724
18 .705
20 .705
22 .706
24 .708
26 .711
28 .714
30 .718
32 .722
34 .728
36 .734
38 .742
40 .75
42 .759
44 .77
46 .781
48 .793
50 .807
52 .821
54 .835
56 .851
58 .866

FREQUENCY = 2000000

ANGLE SQ.ROOT T2

0 .855
2 .856
4 .86
6 .867
8 .877
10 .889
12 .906
14 .928
16 .903
18 .953
20 .974
22 .99
24 .998
26 .998
28 .998
30 .968
32 .942
34 .912
36 .882
38 .856
40 .834
42 .818
44 .809
46 .808
48 .813
50 .825
52 .844
54 .867
56 .893
58 .92



FREQUENCY = 3000000

ANGLE SQ.ROOT T2

0	.158	*
2	.159	*
4	.159	*
6	.16	*
8	.161	*
10	.163	*
12	.165	*
14	.167	*
16	.208	*
18	.194	*
20	.204	*
22	.22	*
24	.243	*
26	.274	*
28	.317	*
30	.378	*
32	.462	*
34	.58	*
36	.732	*
38	.89	*
40	.986	*
42	.995	*
44	.964	*
46	.94	*
48	.94	*
50	.962	*
52	.99	*
54	.998	*
56	.96	*
58	.881	*

FREQUENCY = 4000000
ANGLE SQ.ROOT T2

0 .066	*
2 .066	*
4 .066	*
6 .066	*
8 .066	*
10 .066	*
12 .066	*
14 .064	*
16 .101	*
18 .08	*
20 .083	*
22 .089	*
24 .099	*
26 .113	*
28 .133	*
30 .164	*
32 .21	*
34 .286	*
36 .415	*
38 .629	*
40 .89	*
42 .998	*
44 .991	*
46 .999	*
48 .959	*
50 .764	*
52 .54	*
54 .388	*
56 .295	*
58 .238	*

FREQUENCY = 5000000

ANGLE SQ.ROOT T2

0	.041	*
2	.041	*
4	.04	*
6	.04	*
8	.04	*
10	.039	*
12	.038	*
14	.036	*
16	.077	*
18	.05	*
20	.051	*
22	.055	*
24	.061	*
26	.072	*
28	.087	*
30	.111	*
32	.152	*
34	.227	*
36	.381	*
38	.694	*
40	.979	*
42	.999	*
44	.924	*
46	.567	*
48	.311	*
50	.191	*
52	.131	*
54	.098	*
56	.078	*
58	.064	*

FREQUENCY = 6000000

ANGLE SQ.ROOT T2

0 .033	*
2 .033	*
4 .032	*
6 .031	*
8 .031	*
10 .03	*
12 .029	*
14 .026	*
16 .08	*
18 .04	*
20 .04	*
22 .044	*
24 .049	*
26 .058	*
28 .073	*
30 .098	*
32 .144	*
34 .244	*
36 .501	*
38 .944	*
40 .999	*
42 .752	*
44 .316	*
46 .154	*
48 .09	*
50 .06	*
52 .043	*
54 .033	*
56 .027	*
58 .023	*

FREQUENCY = 7000000

ANGLE SQ.ROOT T2

0 .033	*
2 .033	*
4 .032	*
6 .031	*
8 .03	*
10 .029	*
12 .027	*
14 .023	*
16 .116	*
18 .041	*
20 .04	*
22 .043	*
24 .048	*
26 .058	*
28 .074	*
30 .104	*
32 .166	*
34 .329	*
36 .812	*
38 .994	*
40 .781	*
42 .255	*
44 .103	*
46 .058	*
48 .036	*
50 .024	*
52 .018	*
54 .013	*
56 .011	*
58 .009	*

FREQUENCY = 8000000

ANGLE SQ.ROOT T2

0 .046	*
2 .045	*
4 .044	*
6 .042	*
8 .039	*
10 .036	*
12 .033	*
14 .025	*
16 .277	*
18 .055	*
20 .051	*
22 .053	*
24 .059	*
26 .069	*
28 .089	*
30 .128	*
32 .221	*
34 .529	*
36 .994	*
38 .999	*
40 .349	*
42 .112	*
44 .051	*
46 .028	*
48 .017	*
50 .012	*
52 .008	*
54 .006	*
56 .005	*
58 .004	*

Figure 1 gives the coordinate system for the liquid crystal cell. The origin is at the first glass-liquid crystal interface for the initial matrix calculation and is moved for the final matrix calculation to the lower glass-fluid B interface.

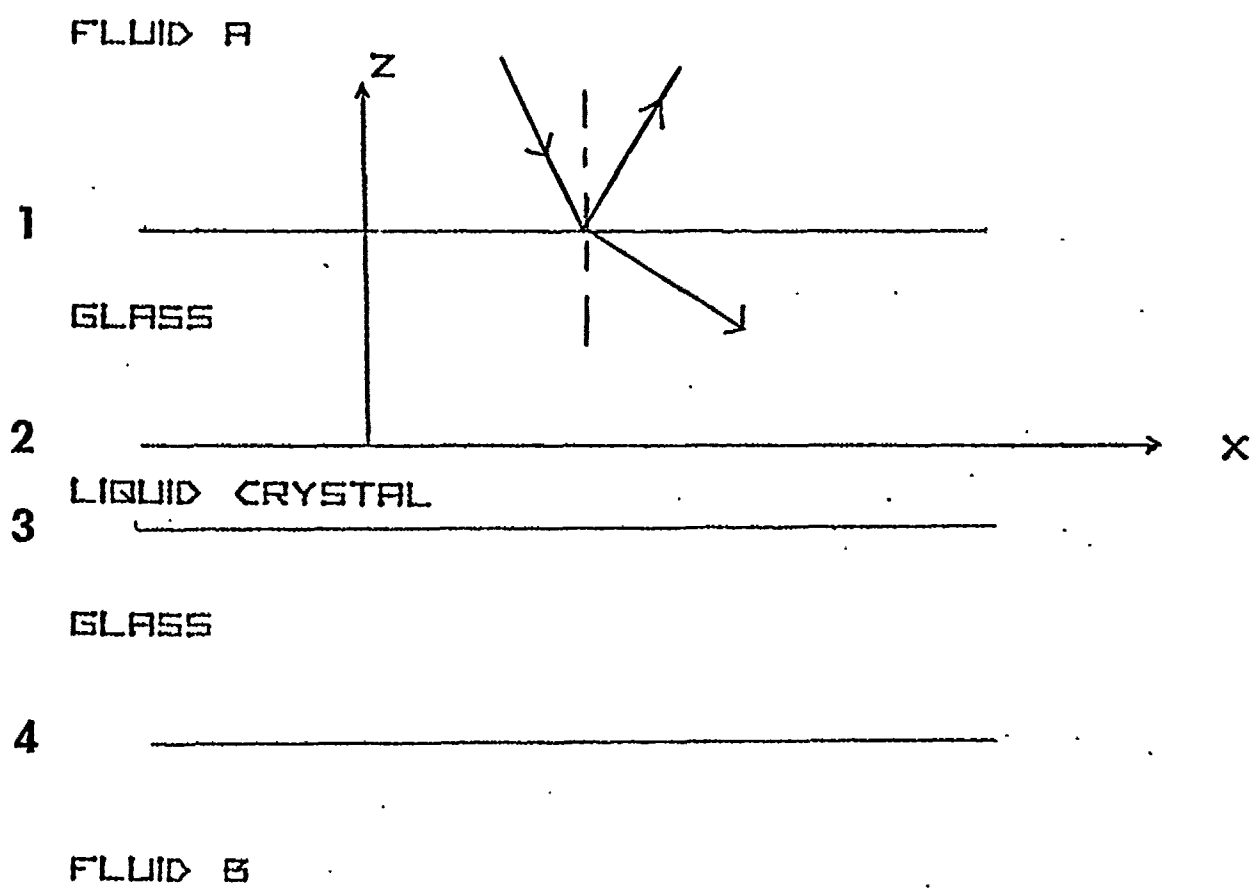


Figure 2 is a graph of the ratio of voltages from the hydrophone with and without a single sheet of 1.6 mm thick glass as a function of angle. Therefore, this graph shows the acoustic transmission of the glass as a function of angle. The crosses are experimental points. The solid line is from Equation 67 for $|D|$. Since each factor in the equation is measured there are no adjustable parameters used to induce the fit. Therefore, the graph represents a severe testing of the theory. For this graph the thicker glass cell is used and a frequency of 0.858 MHz. No correction is made for the finite acceptance angle of the hydrophone.

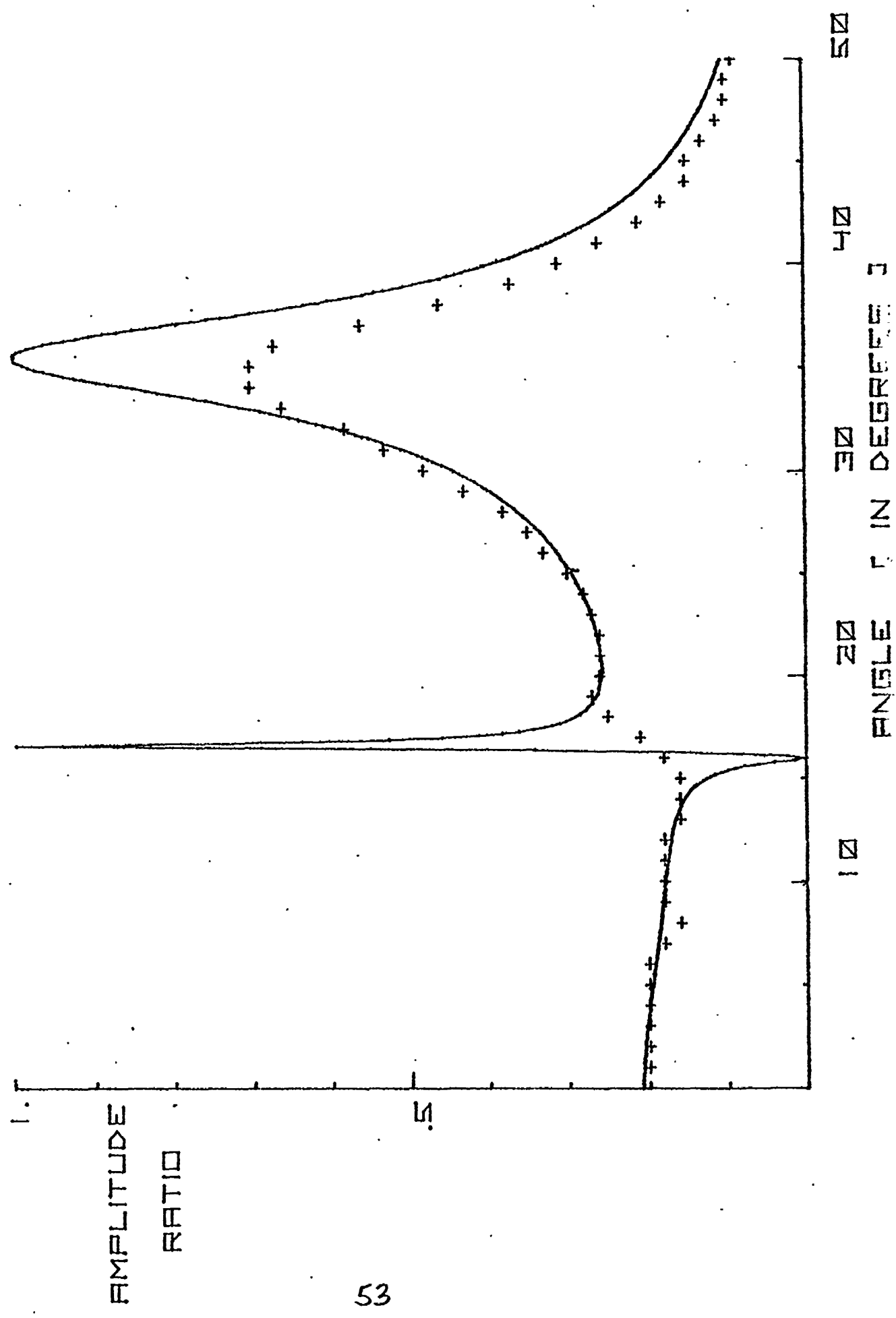


Figure 3 is identical to Figure 2 only correction is made for the finite acceptance angle of the hydrophone.

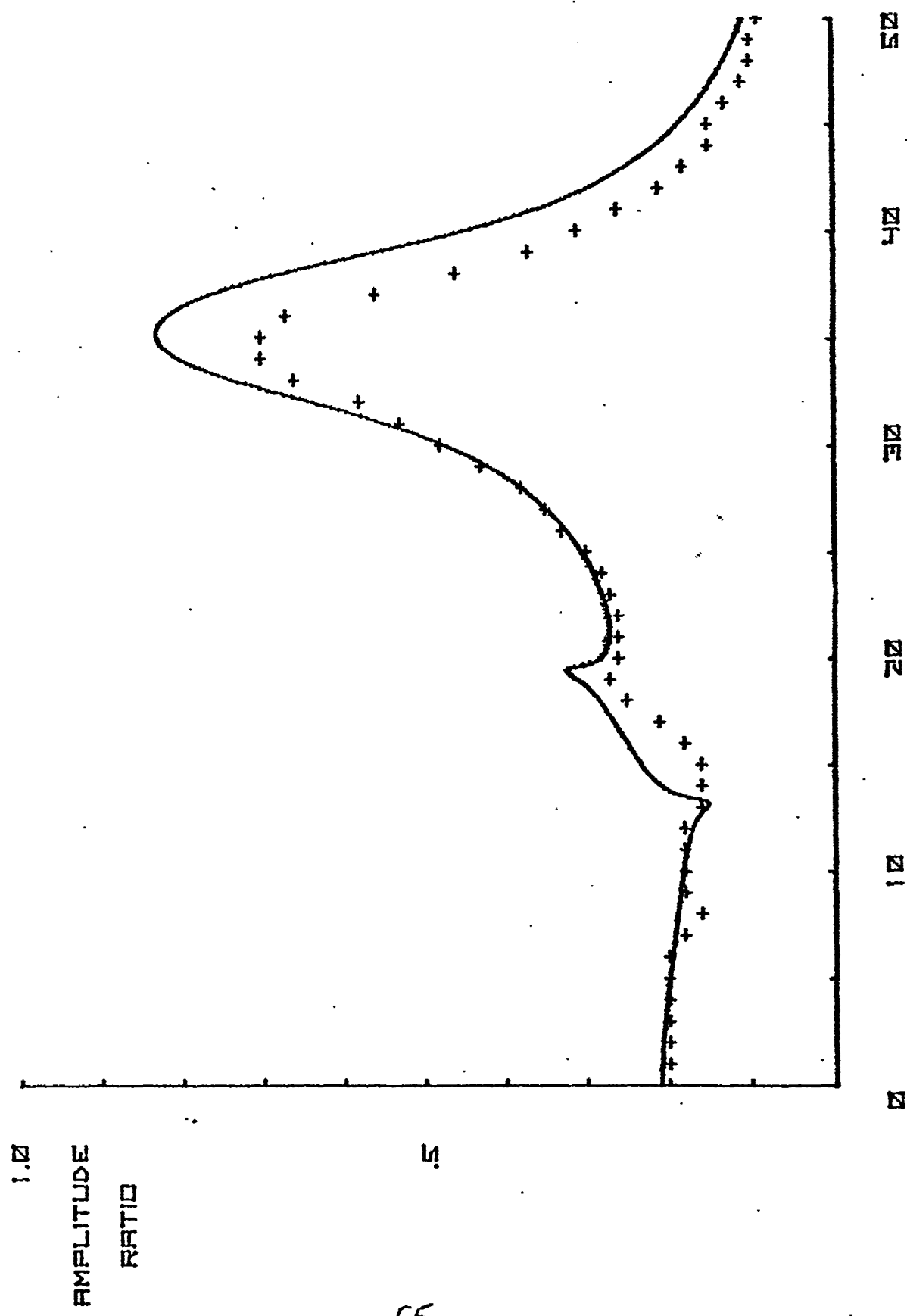


Figure 4 is a graph of the ratio of voltages from the hydrophone with and without a single sheet of 0.146 mm thick glass as a function of angle. The frequency is 0.857 MHz.

ANGLE Γ IN DEGREES 3

50
40
30
20
10

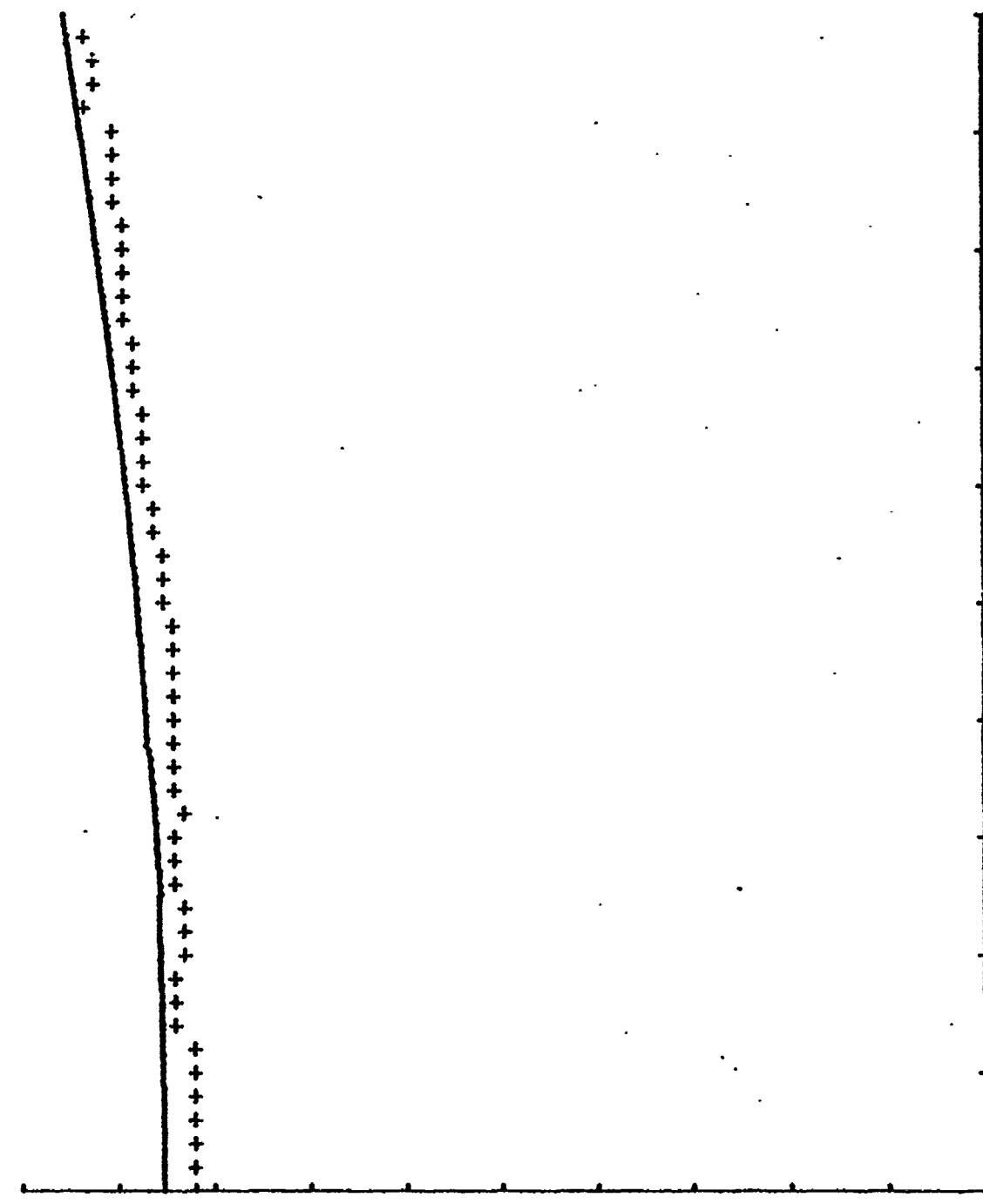


Figure 5 is a graph of acoustic transmission through a liquid crystal cell made of the 1.6 mm thick glass as a function of incident acoustic angle. The acoustic transmission is measured as the ratio of voltage from the hydrophone with and without the presence of the liquid crystal cell. The solid line is the theoretical value of $|D|$ from Equation 67. The crosses are the measured values of acoustic transmission. The filled circles are measured values of transmitted light intensity via the acousto-optic effect using arbitrary linear units. It should be noted that the maximum light intensity occurs at the incident angle for maximum acoustic transmission.

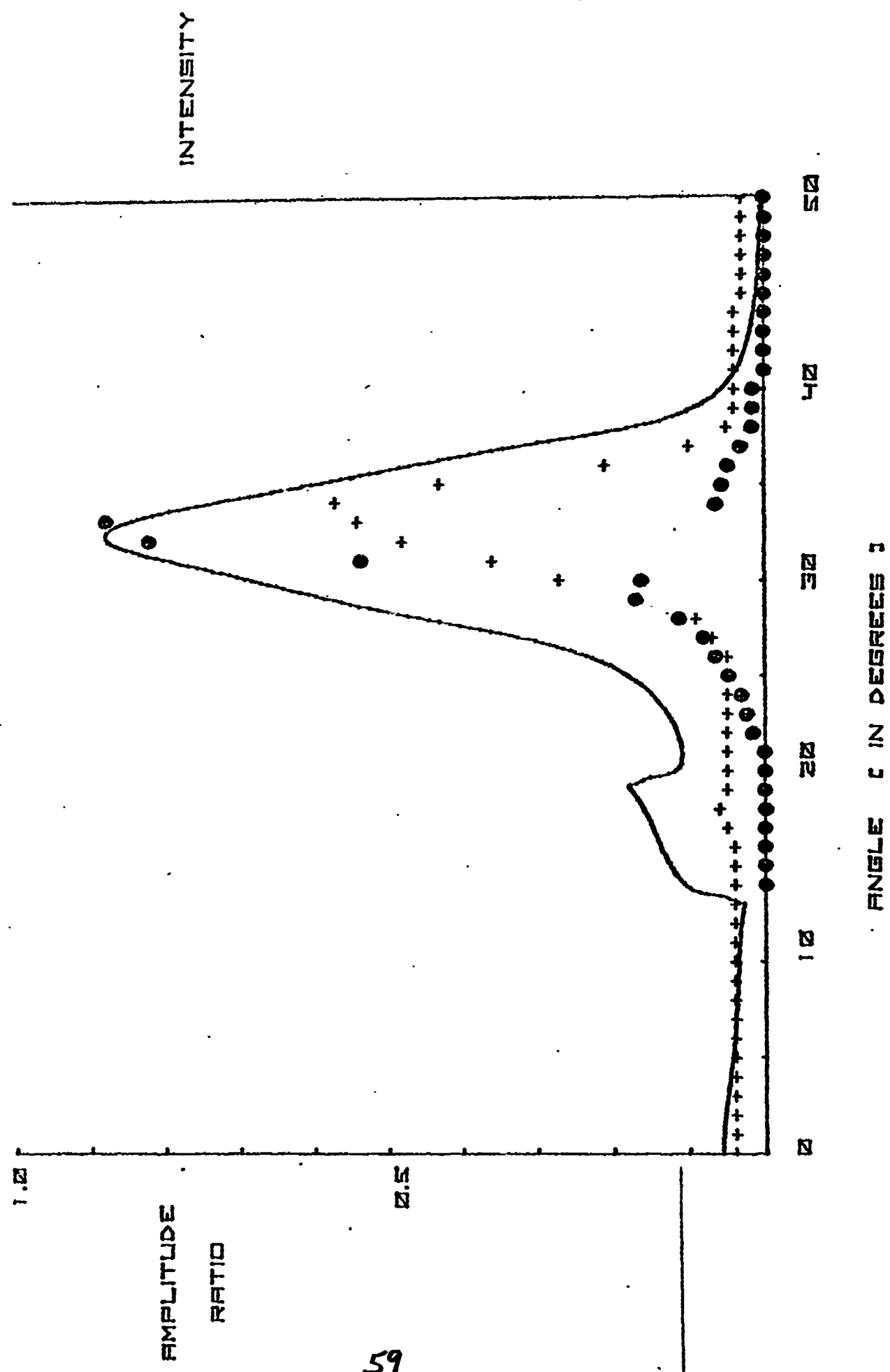


Figure 6 is a graph of acoustic transmission as a function of acoustic frequency. The solid line is the theoretical value from Equation 67. The crosses are the experimental values. There are no adjustable parameters used to induce the fit since each parameter in Equation 67 is known or measured. A liquid crystal cell made of 1.6 mm thick glass is used for these results.

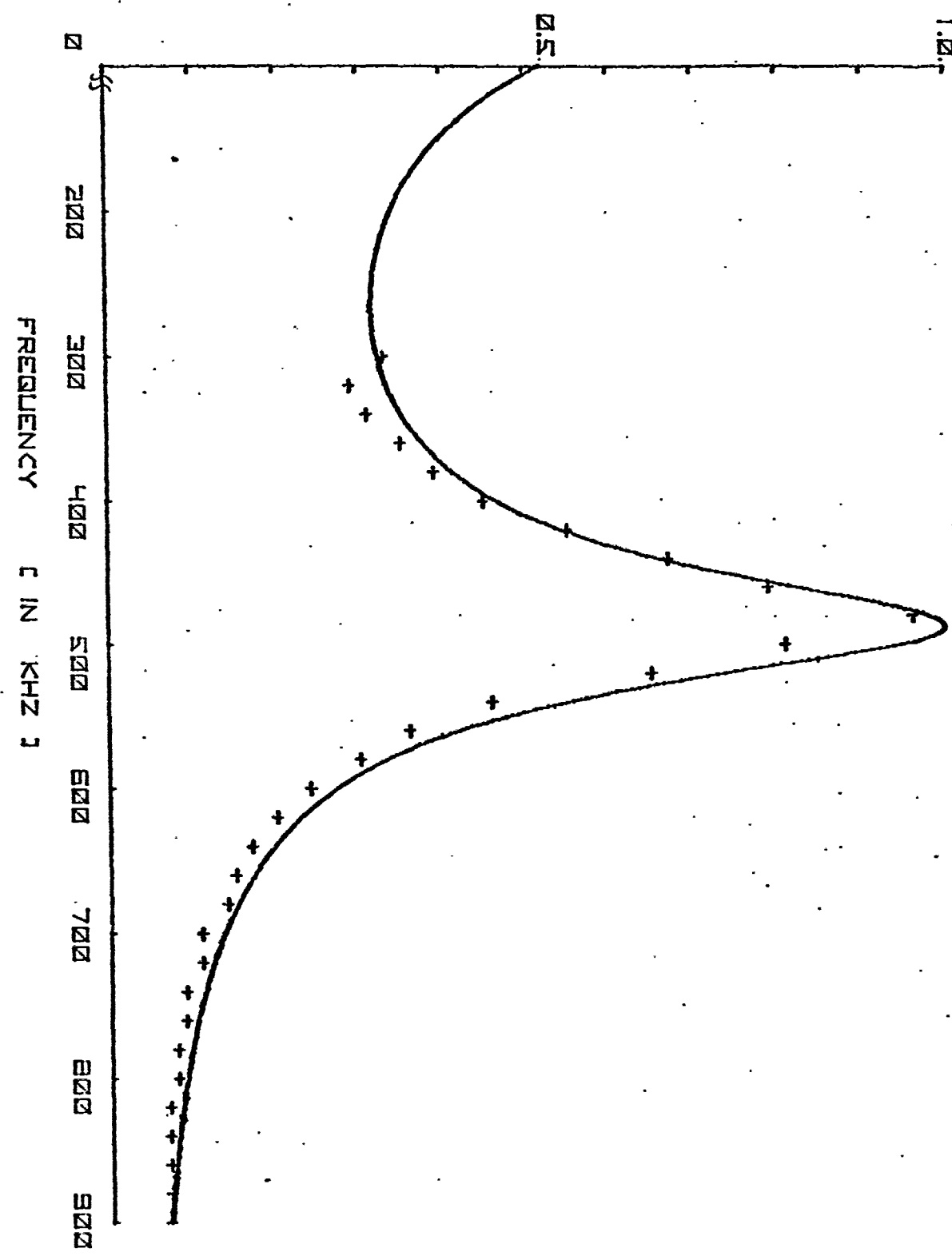


Figure 7 is similar to Figure 5 only the liquid crystal cell is constructed of thinner glass, 0.0146 mm thick. The filled circles represent measured values of transmitted light intensity via the acousto-optic effect.

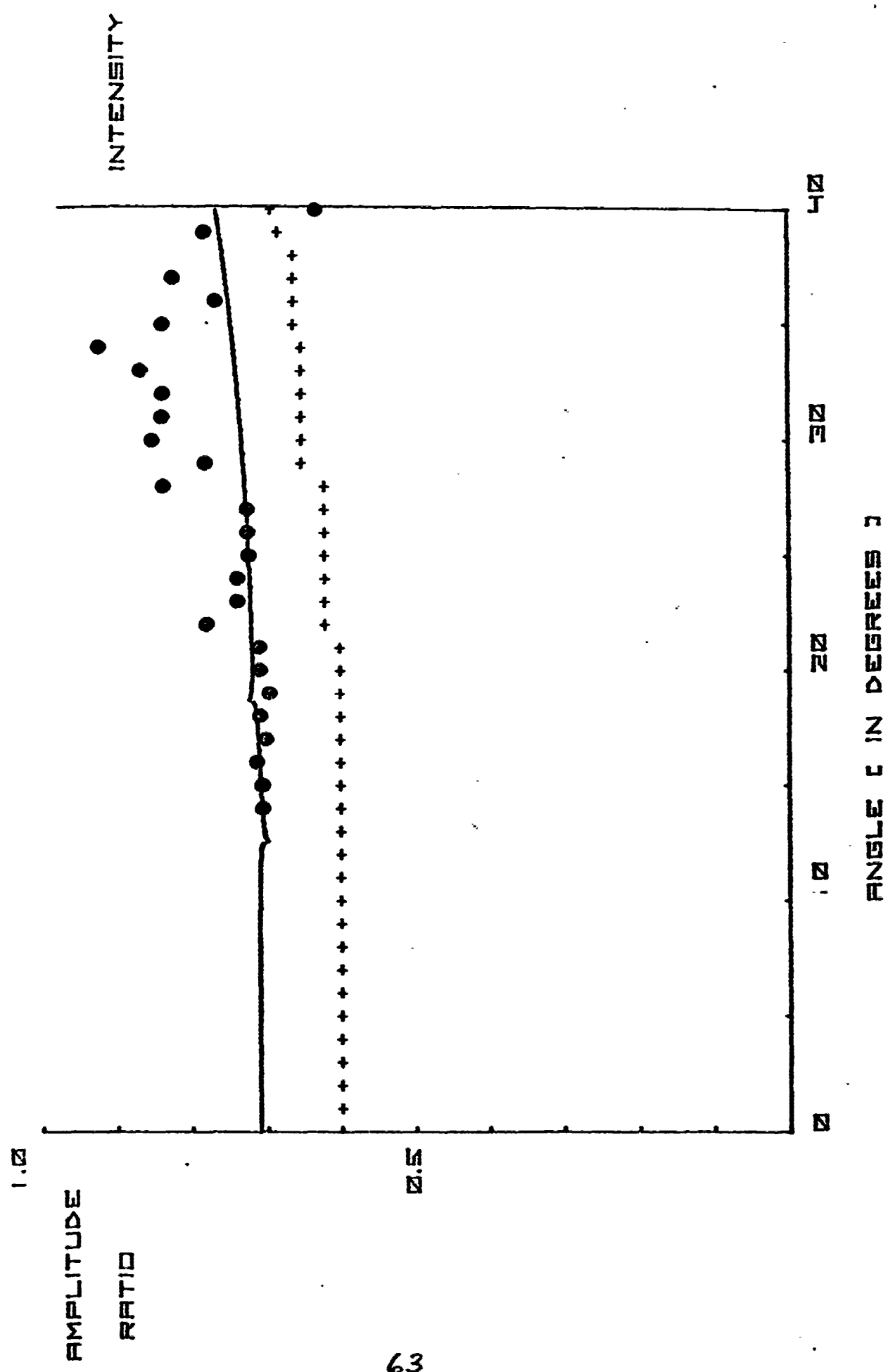


Figure 8 is a series of pictures of the liquid crystal while excited by an ultrasonic wave. The spacing between the resulting vertical lines is seen to decrease with increasing acoustic angle. The angle of incidence for each picture is:

- A. zero degrees
- B. four degrees
- C. twelve and one half degrees
- D. thirteen degrees
- E. negative seventeen degrees (from the right rather than left)
- F. thirty three degrees



A



B



C



D



E



F

Figure 9 is a graph of the distance between the lines such as those shown in Figure 8 as a function of incident angle. The solid line is the fit from Equation 69.

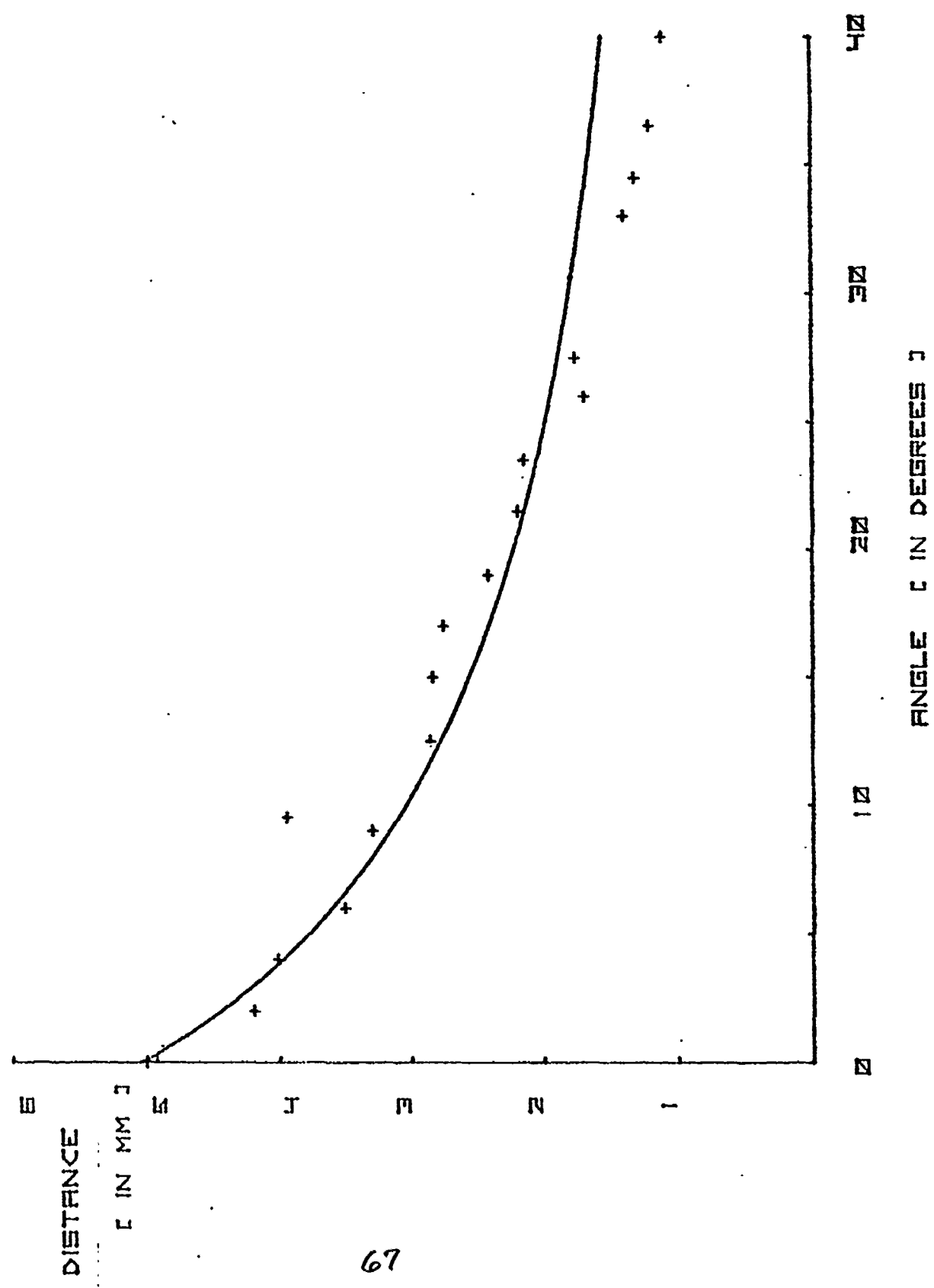


Figure 10 is a sketch of the phase angle of one liquid crystal glass surface with respect to the other versus incident wave angle for a liquid crystal cell constructed of 1.6 mm thick glass. Equation 70 is used for these values.

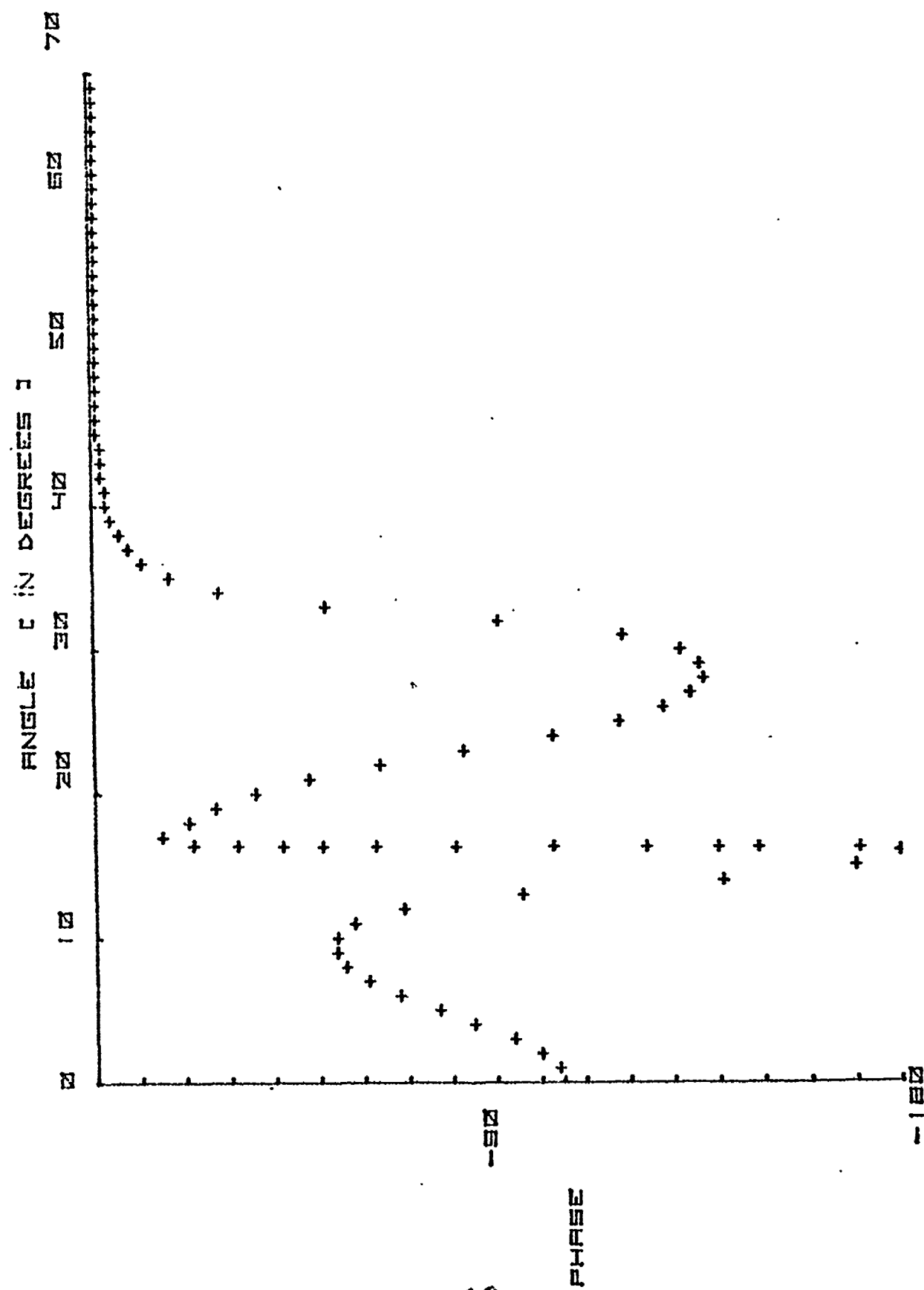


Figure 11 is similar to Figure 10 only for a cell made with 0.0145 mm thick glass.

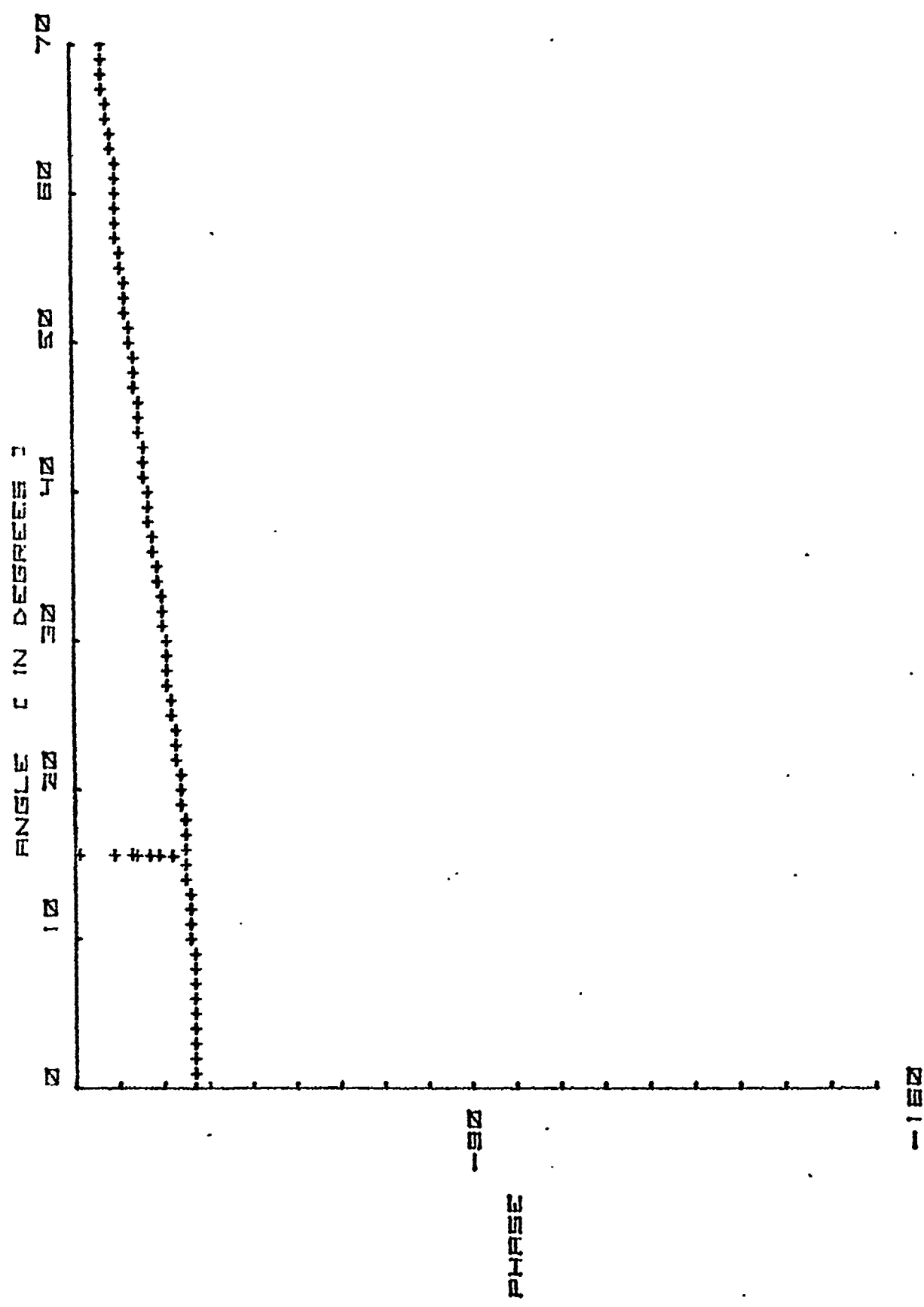


Figure 12 is a graph of acoustic transmission from Equation 67 as a function of liquid crystal layer thickness for a cell of 1.5 mm thick glass. A frequency of 1 MHz and incident angle of zero degrees is used.

NEMATIC THICKNESS t IN MICROMETERS 2

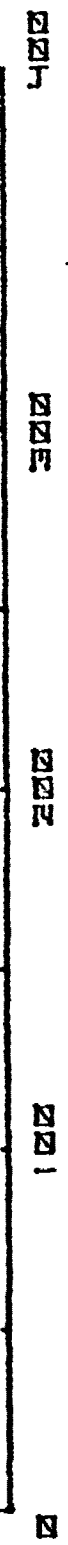
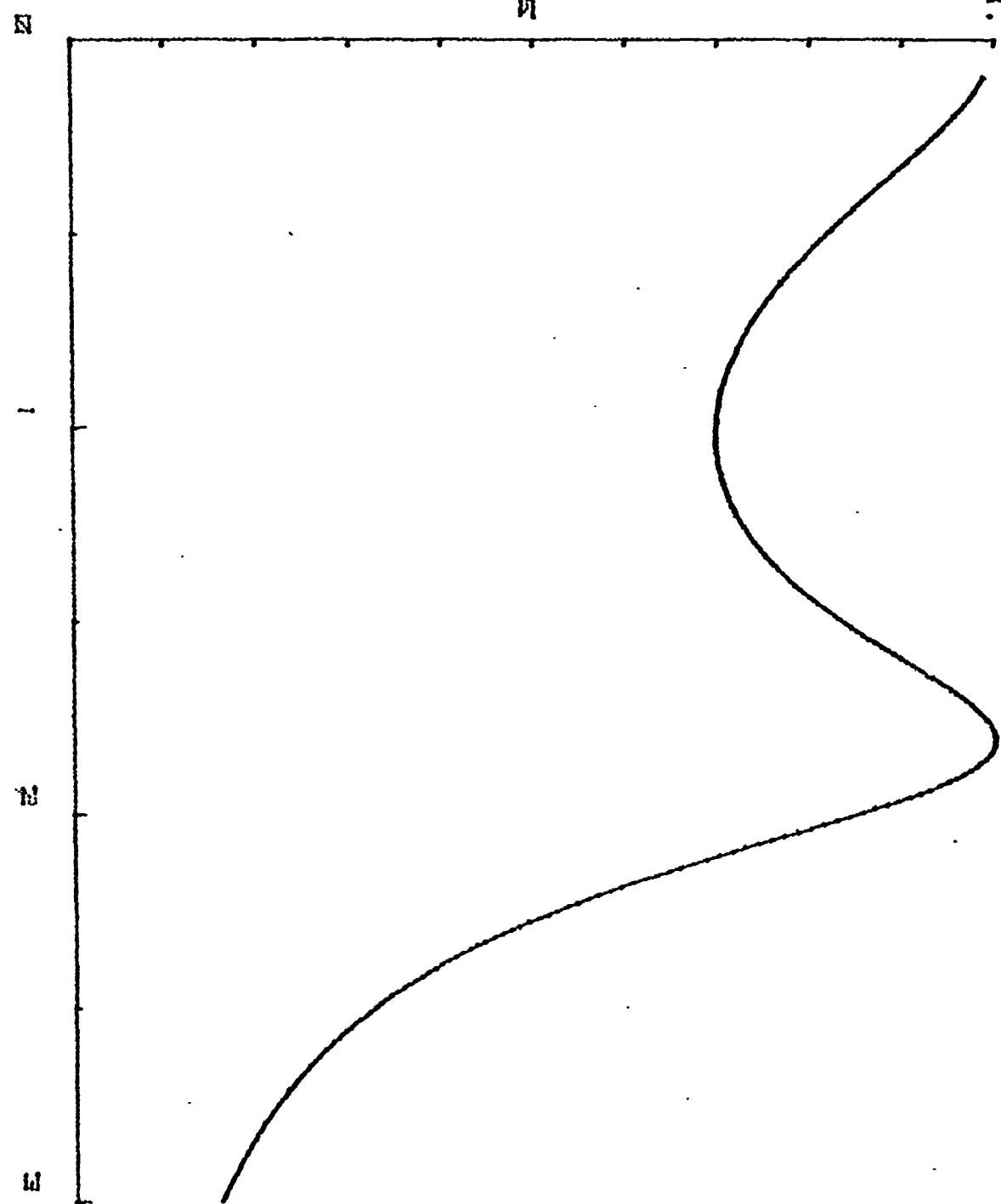


Figure 13 is the acoustic transmission for a cell made with 0.0145 mm thick glass versus frequency.

ДЕТЕКТОРЫ В ИК МН



ДЕТЕКТОРЫ
ИК МН